

Polystyrene-based plastic scintillator for n/γ -discrimination

*P.N.Zhmurin, V.N.Lebedev, V.D.Titskaya, A.F.Adadurov,
D.A.Elyseev, V.N.Pereymak*

Institute for Scintillating Materials, STC "Institute for Single Crystals",
National Academy of Sciences of Ukraine, 60 Lenin Ave., 61001 Kharkiv,
Ukraine

Received March 11, 2014

Polystyrene-based scintillator (PS) with 2-phenyl-5-(4-*tert*-butylphenyl)-1,3,4-oxadiazole or 2,5-di-(3-methylphenyl)-1,3,4-oxadiazole is proposed for pulse-shape n/γ -discrimination. This scintillator have improved mechanical properties, long operational time and high n/γ -discrimination parameter FOM (1.49 and 1.81 in a wide energy region), so obtained PS can be used as detectors of fast neutrons in the presence of gamma radiation background.

Пластмассовые сцинтиллятор на основе полистирола с добавками 2-фенил-5-(4-*трет*-бутилфенил)-1,3,4-оксадиазола или 2,5-ди-(3-метилфенил)-1,3,4-оксадиазола предложены для n/γ -разделения по форме импульса. Эти сцинтилляторы имеют высокие механические свойства, долговременную стабильность и высокие параметры n/γ -разделения FOM (1.49 и 1.81 в широком диапазоне энергии), и, поэтому могут быть использованы в качестве детекторов быстрых нейтронов в присутствии гамма фона.

Пластмасовий сцинтилятор на основі полістиролу для n/γ -розділення.
П.М.Жмурін, В.М.Лебедев, В.Д.Тицька, О.Ф.Ададуров, Д.А.Єлисеєв, В.М.Переїмак.

Пластмасові сцинтилятори на основі полістиролу с домішками 2-фенил-5-(4-*трет*-бутилфенил)-1,3,4-оксадіазолу або 2,5-ді-(3-метилфеніл)-1,3,4-оксадіазол запропоновані для n/γ -розділення за формою імпульсу. Ці сцинтилятори мають високі механічні властивості, довгочасову стабільність і високі параметри n/γ -розділення FOM (1.49 і 1.81 у широкому діапазоні енергії), і можуть бути використані у якості детекторів швидких нейтронів на фоні γ -випромінювання.

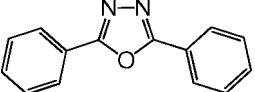
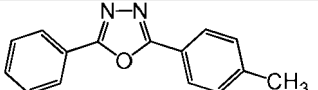
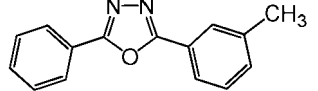
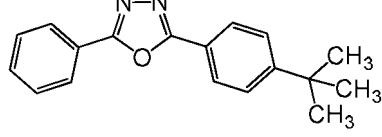
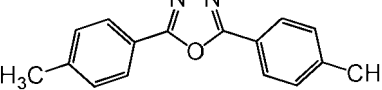
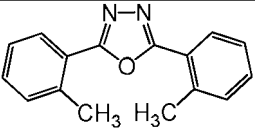
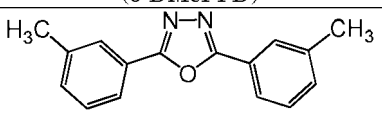
1. Introduction

Zaitseva et al. [1] were first to describe the polyvinyl plastic scintillator (PS) for pulse-shape discrimination (PSD) of fast neutrons and γ -quanta. This scintillator have discrimination quality much the same as that of the best liquid scintillators. Its figure of merit (FOM) is 3.31, compared with $FOM = 3.21$ of the commercially available liquid scintillator EJ-301. The high quality of n/γ discrimination was achieved by the high content of an activator in the PS material (30 wt %

of 2,5-diphenyloxazole (PPO)), which increases the probability of annihilation of excited triplet-triplet states up to values specific for liquid scintillators and stilbene single crystals.

In the present work we studied properties of PS analogous described in [1], but with polystyrene as a base. We made PS samples with 20, 30 and 36 wt.% PPO as an activator, and 0.1 wt % of POPOP as a wave length shifter. It was found that this material is very soft and it is difficult to machine. So the aim of the present work was creating the

Table 1. Melting temperature T_{melt} and solubility of alkyl derivatives 2,5-diphenyl-1,3,4-oxadiazole in polystyrene under $T = 293^{\circ}\text{C}$

Activator number	Activator's name and formulae	$T_{melt}^{\circ}\text{C}$	Solubility wt %
1	 2,5-diphenyl-1,3,4-oxadiazole (PPD)	138	10
2	 2-phenyl-5-(p-tolyle)-1,3,4-oxadiazole (p-MePPD)	125	15
3	 2-phenyl-5-(m-tolyle)-1,3,4-oxadiazole (m-MePPD)	115	15
4	 2-phenyl-5-(4-tert-butylphenyl)-1,3,4-oxadiazole (tert-BuPPD)	95	40
5	 2,5-di-(4-methylphenyl)-1,3,4-oxadiazole (p-DMePPD)	175	4
6	 2,5-di-(2-methylphenyl)-1,3,4-oxadiazole (o-DMePPD)	125	8
7	 2,5-di-(3-methylphenyl)-1,3,4-oxadiazole (m-DMePPD)	85	40

PS with improved mechanical strength and suited for n/γ discrimination.

2. Experimental

To achieve the goal we have chosen such activator substance which has high solubility in polystyrene and, at the same time, has minimal influence on mechanical properties of a polymer matrix. The most important parameter of the commonly used PS is their scintillation efficiency, its maximum being achieved with a small activator content (1.5–2.0 wt. %). Conventional content of the PS is *p*-terphenyl and diaryl substituted of oxazole and oxadiazole [2]. Insert-

ing polar groups to these systems or expanding the π -electron system besides required change of the spectral characteristics often causes decreasing of solubility to some weight percents. Therefore, the search for activators with high solubility is actually limited by alkyl and diaryl derivatives of oxazole and oxadiazole, because their inserting in aromatic fluorophores can significantly increase their solubility in such a nonpolar organic medium as polystyrene.

From the point of view of synthesis ease and components availability, diaryl substituted oxadiazole with alkyl groups were selected as the model compounds.

Table 1 shows the set of synthesized activators which are alkyl derivatives of 2,5-diphenyl-1,3,4-oxadiazole, as well as their melting temperatures and solubility in polystyrene under the room temperature. The set of experimental samples was obtained by radical thermal polymerization of styrene with different concentrations of the activators. The activator's solubility was determined as its concentration which leads to build-up of small parts of undissolved substance.

It is seen in Table 1 that solubility of the studied compounds in polystyrene increases with the decrease of the melting temperature. Relatively small melting temperature (95 and 85°C) and simultaneously high solubility (40 wt. %) have only two compounds — *tert*-BuPPD and *m*-DMePPD (Table 1, comp. 4 and 7), which were used later as activators for the studied PS. For comparison we also made PS with PPO. All PS also have 0.1 wt. % of 1,4-di-(2-(5-phenyloxazolyl))-benzene (POPOP) as wave-length shifter. The PS samples with different content were obtained by mean of thermal polymerization of oxygen-free luminescent additives solution in styrene. Required quantities of activator and shifter were placed in a glass ampoule of 25 mm diameter. Then the fresh distilled styrene was added to 50 g total mass. To achieve the total solution, the ampoule was heated to 80°C and blown by argon for 10 min to remove dissolved oxygen. The ampoule was sealed and heated in a thermostat at 155°C for 7 days. Then the thermostat was cooled with 5°C/h rate to 40°C, the ampoule was removed, cooled to the room temperature and the PS blank was extracted. These blanks were machined to obtain PS samples as polished cylinders of 25 mm diameter and 15 mm height.

To further study the samples were made with three different compositions and maximal content of the activators: 40 % *tert*-BuPPD + 0.1 % POPOP; 40 % *m*-DMePPD + 0.1 % POPOP and 36 % PPO + 0.1 % POPOP (below we will use the following abbreviations: 40 % TBPPD, 40 % DMePPD and 36 % PPO, respectively). When the activators content is increased, the softening and clouding of the PS material was observed. Also, zones of undissolved substance and its accumulation on the PS surface were observed. Decreasing the activator's content leads to fast reducing of n/γ -discrimination quality [1].

Vickers micro hardness (HV) of the PS samples was measured by PMT-3 micro hardness meter under 30 g loading.

Scintillation efficiency of the PS samples was determined in scintillation set-up relative to polystyrene-based PS with 2 % of *p*-TP and 0.02 % of POPOP. The samples were irradiated by mono energetic electrons of 975 keV energy from ^{207}Bi source.

The n/γ -discrimination parameter FOM was determined by comparing the total charge of the signal (Q_{total}) and its delayed component (Q_{tail} or Q_{slow}) [3, 4].

Scintillation set-up was consisted of PMT Hamamatsu R1307 and digital oscilloscope Rigol DC1302 (300 MHz, 2 GS/s, 8 bit vertical resolution), controlled by the computer.

The PS studied were wrapped with PET light reflecting film of 0.2 mm thickness [4] and placed on the PMT input window with optical contact. Fast neutrons and γ -quanta of Pu-Be source, are registered after passing through the lead plate of 20 mm thickness. To increase the vertical resolution, a signal from PMT anode was applied to both channels of the oscilloscope. Under the input resistance of the first and second channels of 51 Ω and 1 M Ω , respectively, and sensitivity of 100 mV/div and 2 mV/div, respectively, the resulting vertical resolution appears to be 13 bit. Scanning rate was 50 ns/div, single time-base trigger was run on the first channel with 6 mV threshold. Digital data from the oscilloscope swapping buffer were put to the PC through a USB-port. Data processing code performed reconstruction of PMT input pulse shape by means of combining the signals from the both channels. Then areas of the whole pulse S_{total} and its delayed component S_{tail} in [V·ns] units were calculated. As far the charge Q is proportional to the pulse area S , then Q_{total} and Q_{tail} can be expressed in [V·ns] or arbitrary units.

Q_{tail} and Q_{total} were determined in 40–400 ns and 10–400 ns intervals, respectively. The both intervals were measured from the maximum of the PMT signal [4]. Q_{tail} and Q_{total} values were collected in the output file for each detected pulse.

The n/γ -discrimination parameter FOM is usually determined for selected interval ΔQ_{total} from the pulse distribution in Q_{slow} [4] or $R = Q_{slow}/Q_{total}$ [1] by the following equation:

$$FOM = \frac{S}{\delta_{\text{gamma}} + \delta_{\text{neutron}}}, \quad (1)$$

where S — is separation between neutron and gamma peaks, δ_{gamma} and δ_{neutron} — are full width at half maximum of the corresponding peaks [6].

The interval ΔQ_{total} is selected according to the energy range of the particles for which FOM is calculated. As far as two kind of particles are registered (neutrons by recoil protons and gamma-quanta by Compton electrons), then the Q_{total} signal from each particle is typically expressed in units of electron-equivalent energy E_{ee} (keVee, MeVee). Energy scale calibration is usually made by means of gamma radiation of various radioactive sources from the position of the Compton edge.

More accurate way is the calibration by means of mono energetic electrons. This method can be applied when the electrons are totally absorbed in a PS. To this end the PS input window must be thin enough, to attenuate electrons only slightly, while the PS thickness must be large for total absorption of electrons. For example, if electrons of 1 MeV energy are used for spectrometer calibration, their range in polystyrene being 4.48 mm [7], then the PS sample must be of not less than 5 mm thick. The PS studied in the present work satisfied these requirements. The input window (PET light reflecting film of 0.2 mm) was thin enough while the PS thickness (15 mm) was sufficiently large to absorb electrons of 3 MeV energy.

In the present work the calibration of the electron-equivalent energy was made by mono energetic electrons of internal conversion from ^{207}Bi (482 keV and 975 keV) and ^{137}Cs (624 keV) sources.

The calibration procedure of electron-equivalent scale for the PS with 36 % of PPO is illustrated by Fig. 1, which presents distributions of detected electrons in Q_{total} , that is energy spectra of electrons from ^{137}Cs (Fig. 1a) and ^{207}Bi (Fig. 1b) sources. Positions of maxima, corresponding to electrons of E_e energy [(624 keV–42.9 V·ns (^{137}Cs); 482 keV–33.3 V·ns and 975 keV–68.4 V·ns (^{207}Bi)] were determined by Gaussian fitting the peaks. After liner approximation of these data the calibration curve was obtained which relates the electron energy E_e to the pulse area Q_{total} : $E_e(\text{keVee}) = -8.61 + 14.45 Q_{\text{total}}$, (Fig. 1c).

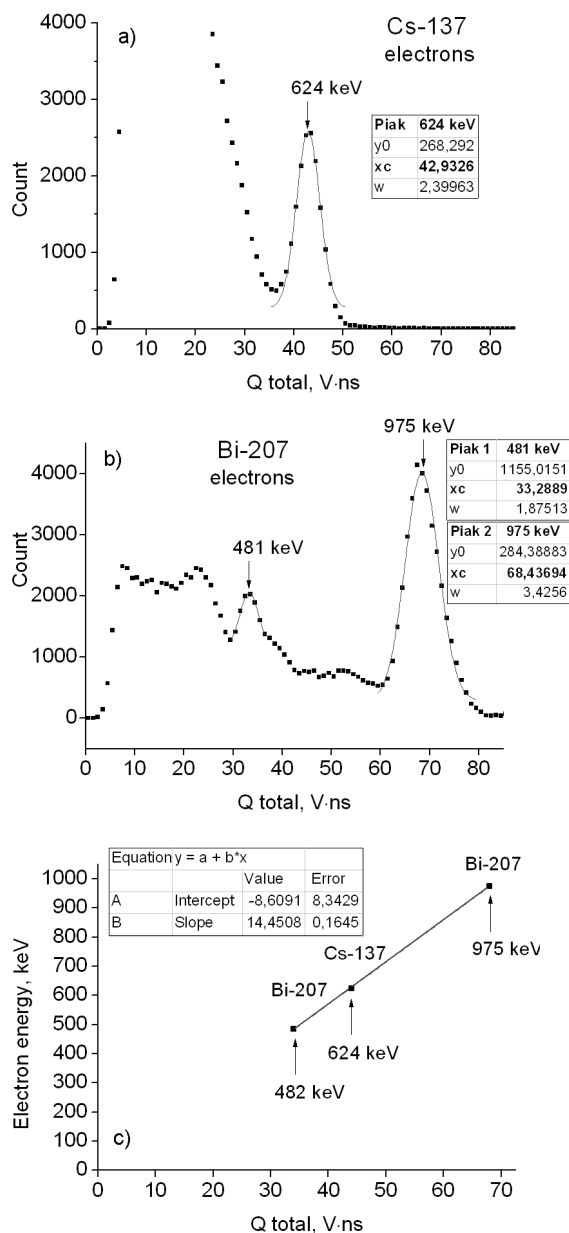


Fig. 1. Calibration of electron equivalent energy scale for PS 36 % PPO. Spectra of ^{137}Cs (a) and ^{207}Bi (b). Linear approximation of electron energy E_e vs Q_{total} (c).

3. Results and discussion

Fig. 2 presents Q_{slow} vs. Q_{total} dependences for three studied PS: 40 % TBPPD (a), 40 % DMePPD (b) and 36 % PPO (c). These data were obtained by registration of fast neutrons and γ -quanta from ^{239}Pu -Be source. Two sets of points are clearly distinguished in all dependences. The set of lower Q_{slow} corresponds to gamma quanta and the set with high Q_{slow} corresponds to neutrons.

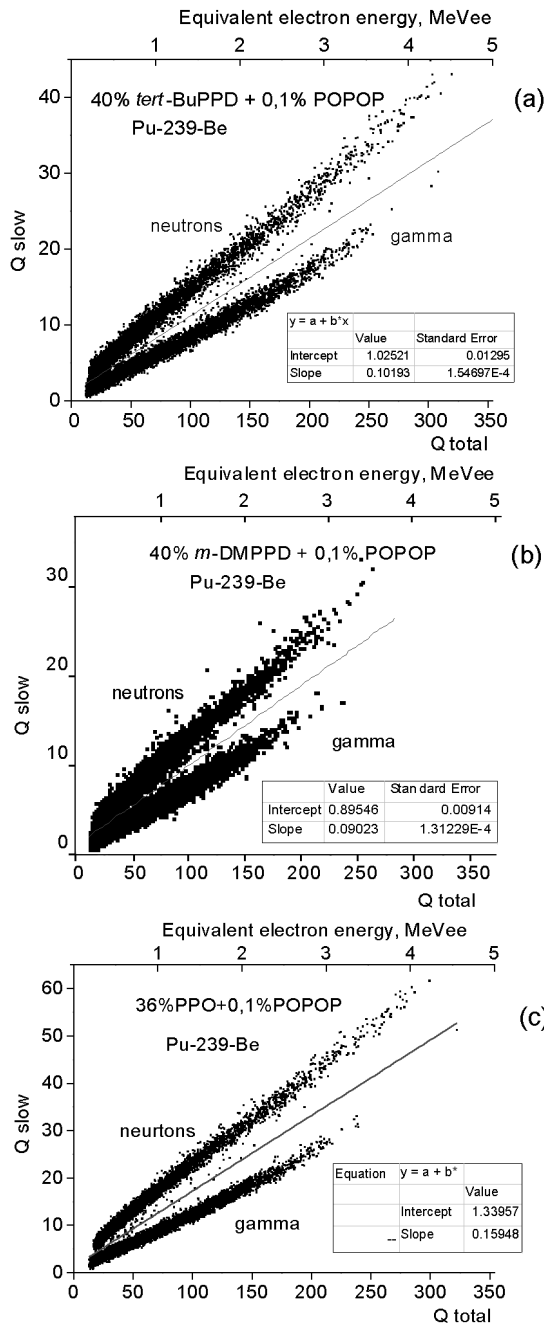


Fig. 2. Q vs Q_{total} for PS with: (a) — 40 % of TBPPD; (b) — 40 % of DMePPD and (c) — 36 % of PPO. Fast neutrons and gamma quanta of $^{239}\text{Pu-Be}$ source.

This illustrates the basic possibility of proposed PS use for n/γ -discrimination.

To quantitative estimation of n/γ -discrimination of the studied PS we determined FOM in different energy regions by the modified method, proposed in [4]. For FOM calculation, authors of [4] used Q_{slow} vs Q_{total} dependence similar to presented in Fig. 2. Then they selected events corre-

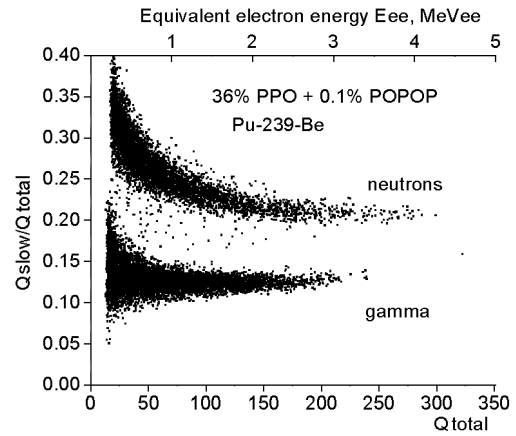


Fig. 3. Q/Q_{total} vs Q_{total} dependence for PS with 36 % PPO, obtained for fast neutrons and γ -quanta of $^{239}\text{Pu-Be}$.

sponding to narrow interval of electron equivalent energies ΔE_{ee} , and plotted distribution of selected events in Q_{slow} . From fitting this distribution by two Gaussians the required parameters were obtained for FOM calculation according to (1). It is obvious that disadvantage of such a method is dependence of obtained FOM on interval width ΔE_{ee} under given E_{ee} , because Q vs Q_{total} dependence is linearly increased function (Fig. 2), and this dependence in Q_{slow} is a projection of events interval ΔQ_{slow} on the axis of ordinates [4].

To eliminate this disadvantage, authors of [1] used Q_{slow}/Q_{total} vs. Q_{total} distribution for FOM determination. This function is practically constant for $E_{ee} \geq 1$ MeV, but rapidly changes in the region of lower energies which is demonstrated in Fig. 3 for the PS with 36 % PPO. Moreover, as it is known, the spread of Q_{slow}/Q_{total} is greater than the spread of Q_{slow} or Q_{total} , which decreases the FOM obtained by this method. Therefore, to FOM calculation we used "normalized" dependence $Q_{slow}/\langle Q_{slow} \rangle$ vs Q_{total} , where $\langle Q_{slow} \rangle = a + b \cdot E_{ee}$ is the center line dividing both sets. The function $\langle Q_{slow} \rangle$ is shown in Fig. 2 as the solid line, dividing sets of experimental points for neutrons and gamma quanta.

$Q_{slow}/\langle Q_{slow} \rangle$ dependence from Q_{total} for the PS with 40 % of TBPPD, 40 % of DMePPD and 36 % of PPO is shown in Fig. 4. It is seen that $Q_{slow}/\langle Q \rangle$ are changed only slightly in the whole diapason of energies of neutrons and gamma quanta of $^{239}\text{Pu-Be}$ source. This allows to reduce influence of ΔE_{ee} on a FOM .

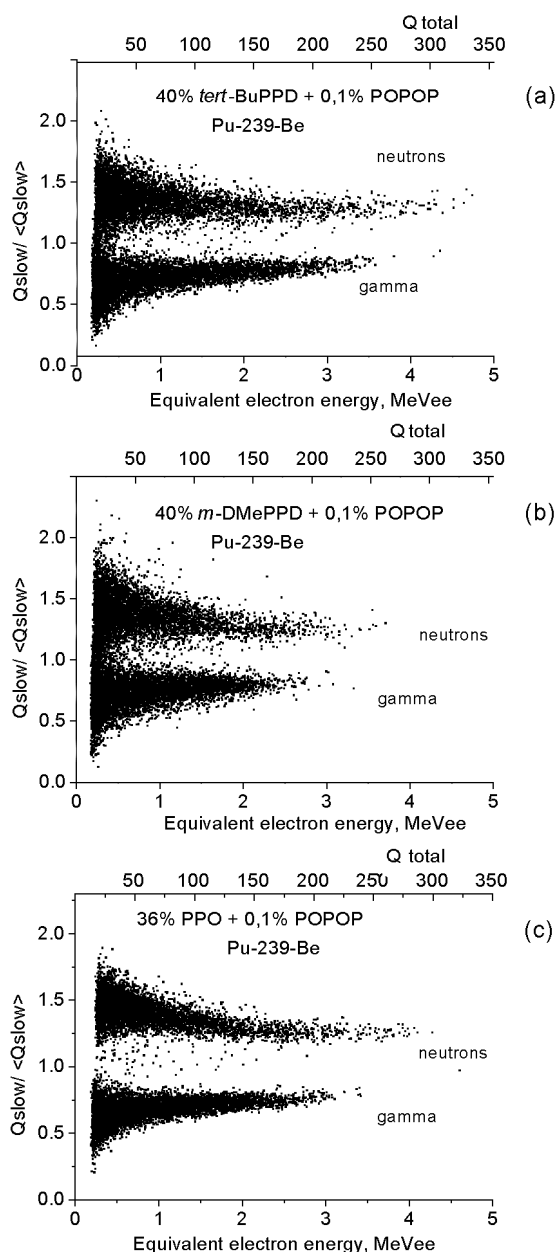


Fig. 4. Dependence $Q/\langle Q_{slow} \rangle$ from Q_{total} for PS with: (a) — 40 % TBPPD; (b) — 40 % DMePPD and (c) — 36 % PPO, obtained for fast neutrons and γ -quanta of ^{239}Pu -Be source.

To obtain FOM , the set of Q_{slow} and Q_{total} pairs was sorted by Q_{total} . Events from $\Delta E_{ee} = E_{ee} + 0.05\%$ were selected and their distribution in $Q_{slow}/\langle Q \rangle$ was plotted. These distributions for the PS with 40 % TBPPD were presented in Fig. 5 for three energy intervals: $\Delta E_{ee} + 5\%$ (0.29–0.31; 0.76–0.84 and 1.9–2.1) MeVee, respectively. Left peaks correspond to gamma quanta, and right ones — to neutrons, the data were obtained for FOM was determined according to (1) after Gaussian fitting of these distribu-

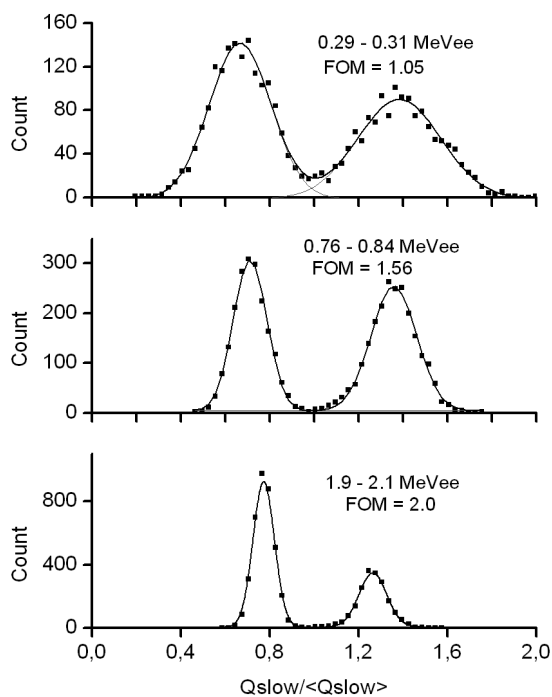


Fig. 5. Distribution of events in Q for PS with 40 % *tert*-BuPPD + 0.1 % POPOP for different intervals of electron equivalent energies $\Delta E_{ee} = E_{ee} + 0.05\%$. Left and right peaks correspond to gamma quanta and neutrons of ^{239}Pu -Be source. Points — experiment, solid lines — Gaussian fitting. For each distribution the interval ΔE_{ee} and calculated FOM are presented.

tions. FOM values for above ΔE_{ee} appears to be 1.05, 1.56 and 2.0, as shown in Fig. 5. The FOM values for other studied PS calculated for different electron equivalent energies E_{ee} , are presented in Table 2 and in Fig. 6.

It is seen in Fig. 6 that quality of the n/γ discrimination is rapidly increases with increasing the energy of detecting particles approximately up to 1 MeVee. Then this increasing is slow down. To statistically significant discrimination of two Gauss distributions, their separation S must satisfy the condition $S > 3(\sigma_{gamma} + \sigma_{neutron})$, where σ is the standard deviation for gamma quanta and neutrons [1]. Substituting these parameters in (1), and taking into account $FWHM \approx 2.36\sigma$, we find $FOM \approx 1.27$. So, statistically significant n/γ -discrimination quality is achieved when $FOM \geq 1.27$.

As it shown in Fig. 6, for PS with 40 % of TBPPD, 40 % of DMePPD and 36 % of PPO this condition is fulfilled for $E_{ee} \geq 0.5, 1.25$ and 0.2 MeVee, respectively. Results of measurements of the relative scintillat-

Table 2. *FOM* values for three studied PS measured for different electron-equivalent energies E_{ee}

E_{ee} , MeVee	<i>FOM</i>		
	40 % TBPPD	40 % DMePPD	36 % PPO
0.3	1.05	0.68	1.54
0.4	1.19	0.82	1.75
0.6	1.43	0.99	2.02
0.8	1.56	1.13	2.24
1	1.67	1.22	2.41
1.5	1.85	1.38	2.75
2	1.99	1.50	2.96
2.5	2.15	1.63	3.23

ing efficiency, microhardness and parameter of n/γ -discrimination for the PS of different content are presented in Table 3. These data show that the scintillating efficiencies of all PS are nearly the same and only about 11 % below that of the standard PS sample with 36 % of PPO (sample 4). But microhardness and *FOM* significantly depend on molecules structure and quantity of the used activator. The microhardness is decreased with *FOM* increasing. The highest microhardness, $HV = 231$ MPa, has the standard PS with lowest content of the activator (2 % *p*-TP). The lowest microhardness, $HV = 21$ MPa, has PS with 36 % of PPO, which molecules do not contain any substituent and therefore have the most simple structure. TBPPD and DMePPD molecules with alkyl substituents have more branched structure compared to PPO (Table 1), which creates high steric difficulties for their diffusion in the polymer. Therefore the PS with 40 % of TBPPD and 40 % of DMePPD have more high microhardness ($HV = 135$ and 73 MPa, respectively), than the PS with 36 % of PPO.

Increase of the activator concentration leads to increase of n/γ -discrimination due to triplet-triplet annihilation. At the same time the microhardness decreases because high concentration of the activator leads to replacing the part of rigid structured polymer matrix by a soft amorphous substance

Table 3. Relative scintillating light yield, microhardness HV , and n/γ discrimination parameter *FOM* of the PS sample of different content

PS number	PS content (polystyrene matrix), wt. %	Rel. LY	%	Microhardness by Vickers HV , MPaa
1	Standard: 2 % of <i>p</i> -terphenyl + 0.05 % POPOP	100	231	<0.5
2	40 % of <i>tert</i> -BuPPD + 0.1 % POPOP	90	135	1.67
3	40 % of <i>m</i> -DMePPD + 0.1 % POPOP	96	73	1.22
4	36 % of PPO + 0.1 % DPA	89	21	2.41

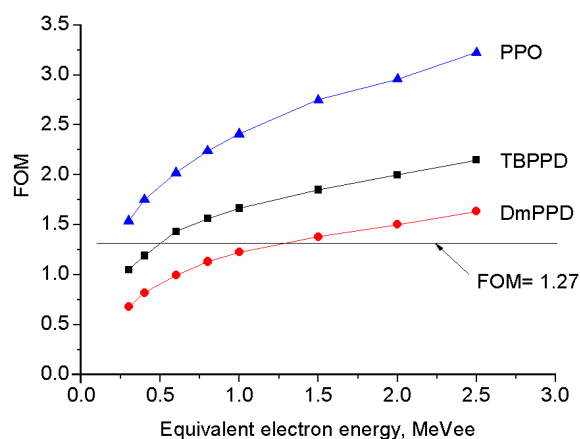


Fig. 6. Dependence of n/γ -discrimination parameter *FOM* on E_{ee} for PS with 40 % of TBPPD, 40 % of DMePPD and 36 % of PPO. The data are obtained for fast neutrons and gamma quanta of ^{239}Pu -Be source. Horizontal curve corresponds to $FOM = 1.27$, for which n/γ -discrimination error is $3(\sigma_{\text{gamma}} + \sigma_{\text{neutron}})$, where σ_{gamma} and σ_{neutron} is the standard deviation for gamma quanta and neutrons distributions.

(plasticization effect). The level of microhardness decreasing depends on affinity of activator substance to the polymer matrix and on the structure of alkyl substituents in its molecule.

So, in the PS with high activator content (up to 40 wt. %) there is a possibility of microhardness increasing by means of activators with high affinity to a polymer matrix and more branching structure of used alkyl substituents because of low mobility of such molecules in a polymer matrix. At the same time, it follows from observed decrease of *FOM* that alkyl substituents create steric difficulties for close approach of the chromophore fragments of the molecule. This reduces the probability of triplet excitations migration thus reducing the probability of triplet-triplet annihilation. As a result, the intensity of the delayed component of scintillation pulse is decreased and the n/γ -discrimination quality is reduced.

But, in spite of some *FOM* reducing, material of polystyrene-based PS for n/γ -discrimination with 40 % *tert*-BuPPD + 0.1 % POPOP is close by its physical and chemical properties to the well-known standard PS UPS-923A [8]. This material as well as that with 40% TBPPD, is well polymerized in large volumes, easily cut and polished, have high transparency and hardness and it is time-stable.

4. Conclusions

The set of activators — alkyl derivatives of diphenyloxadiazole have been synthesized. Their solubility in a polymer matrix has been studied. It is found that two activators, namely, 2-phenyl-5-(4-*tert*-butylphenyl)-1,3,4-oxadiazole and 2,5-

di-(3-methylphenyl)-1,3,4 oxadiazole have more than 40 % solubility. These two activators were used to obtain PS with the high n/γ discrimination and high microhardness.

The capability of n/γ -discrimination of the PS with high concentration of activators was shown.

The parameter of n/γ -discrimination was calculated to be 1.49 and 1.81 for the studied PS. For signals reliable discrimination, *FOM* must be greater than 1.27, so the obtained PS can be used as detectors of fast neutrons in the presence of gamma radiation background.

References

1. N.Zaitseva et al., *Nucl. Instr. and Meth. Phys. Res.*, **A668**, 88 (2012).
2. J.B.Birks, *The Theory and Practice of Scintillation Counting*, Pergamon Press, London (1964).
3. C.L.Morris, *Nucl. Instr. Meth. Phys. Res.*, **137**, 397 (1976).
4. J.H.Heltsley et al., *Nucl. Instr. Meth. Phys. Res.*, **A263**, 441 (1988).
5. S.Nutter et al., *Nucl. Instr. Meth. Phys. Res.*, **A310**, 665 (1991).
6. R.A.Winyard et al., *Nucl. Instr. Meth. Phys. Res.*, **95**, 141 (1971).
7. Stopping Powers for Electrons and Positrons (ICRU report 37; Intern. Commis. on Radiat. Units and Measur.), Bethesda, Maryland, USA (1984).
8. V.G.Senchishin et al., *Semiconductor Physics. Quantum Electronics & Optoelectronics*, **3**, 223 (2000).